The rupture of lipid vesicles near solid surfaces

Annamária Takáts-Nyeste[1] and Imre Derényi[1]

[1]*ELTE-MTA "Lendulet" Biophysics Research Group, Department of Biological Physics, Eötvös University, Pázmány P. stny. 1A, H-1117 Budapest, Hungary*

(Dated: April 24, 2014)

The behavior of lipid vesicles near solid surfaces, despite its scientific and technological significance, is poorly understood. By simultaneously taking into account (i) the dynamics of spontaneous pore opening and closing in surface bound vesicles; (ii) their volume loss via leakage through the pores; (iii) and the propagation of their contact line, we have developed a simple model that can fully describe the detailed mechanism of and provide the necessary conditions for the rupture of vesicles and the subsequent formation of supported lipid bilayers. The predictions of the model are in good agreement with most of the experimental observations.

PACS numbers: 87.16.D-, 87.10.-e, 87.85.J-, 68.15.+e

Biological membranes play key roles in living cells by separating the cell and its organelles from their surrounding media. Supported lipid bilayers (SLBs), i.e., single lipid bilayers anchored to a solid substrate, are frequently used models of biological membranes (both for investigating membrane processes and for biotechnological applications). The most common method of producing SLBs is the spontaneous self-assembly of a continuous bilayer along a solid surface from unilamellar vesicles depositing from solution. Despite the widespread use of SLBs, the mechanism of their formation is still a matter of debate, surrounded by controversial experimental data, mainly due to the sever limitations in observing the fast microscopic events of the adsorption and rupture of individual vesicles. Ensemble techniques, such as quartz crystal microbalance (QCM) [1] or surface plasmon resonance (SPR) [2], indicated that vesicle rupture and SLB formation occur only after a critical vesicle coverage has been reached on the surface. Microscopic techniques, such as fluorescence microscopy (FM) [3], atomic force microscopy (AFM) [4], and cryotransmission electron microscopy (cryo-EM) [5], on the other hand, revealed the occurrence of isolated ruptures of individual vesicles. The FM studies showed that the fraction of ruptured vesicles prior to SLB formation can be as high as 50%. Combined QCM and AFM studies [6] uncovered some discrepancies between the results of these two methods, questioning the reliability of the ensemble techniques. Recent FM studies by Weirich et al. [7] argued against the existence of a critical vesicle density necessary for rupture. Their results suggest that small bilayer patches appear after the rupture of isolated vesicles, and then these patches grow by accelerating both the accumulation and rupture of vesicles at the patch edges. This study reconciles the apparent conflict between the existence of isolated ruptures and the observed critical vesicle coverage for SLB formation, articulating that critical coverage is needed only for efficient bilayer growth (and not vesicle rupture) while nucleation seeds are generated by isolated vesicle ruptures.

Most recently, Andrecka et al. [8] used interferometric scattering microscopy (iSCAT), which allowed them to visualize SLB formation from vesicles at an unprecedented spatial and temporal resolution. They also observed vesicle adsorption, rupture, movement, and a wave-like spreading of bilayer patches. They found that the rate of spontaneous vesicle rupture decreases with vesicle size (in agreement with earlier AFM measurements [4]), and that the close proximity of vesicles does not catalyze spontaneous vesicle rupture, nor does it result in vesicle fusion. The observed wave-like spreading suggests that wave formation is initiated by the spontaneous rupture of individual seed vesicles, and the major role of the critical coverage is to ensure efficient bilayer propagation via inducing vesicle rupture at the bilayer edges. By varying the interaction potential between the vesicles and the substrate they noticed that stronger interaction leads to faster vesicle rupture. This is consistent with the often observed behavior that while on certain substrates (such as glass and mica) vesicle adsorption is followed by SLB formation, on other substrates (e.g. TiO_2, oxidized Pt, oxidized Au) vesicles adsorb but remain intact [1]. Similarly, varying the interaction strength by using charged lipids can lead to either no absorption, or the formation of a stable vesicular layer, or the decomposition of adsorbed vesicles into SLB [9].

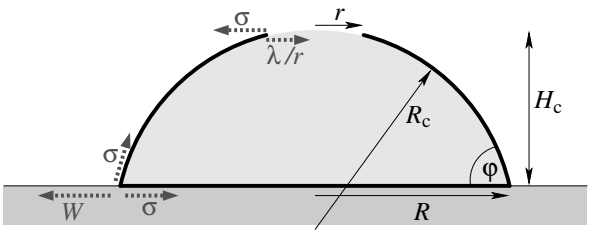

FIG. 1. Schematic picture of a surface bound cap-shaped vesicle in the limit of strong adhesion, with a pore at the top.

The above experimental results suggest that the key step in SLB formation is the rupture of individual vesicles. This is, however, a complex process involving membrane pore formation, membrane dynamics, as well as hydrodynamics, which have never been integrated into a single self-consistent theoretical description. Our goal here is to understand the rupture process of individual vesicles by constructing a simple coarse-grained model that simultaneously takes into account the dynamics of spontaneous pore opening and closing along the membrane; the volume loss of the vesicle via leakage through the pores; and the propagation of the contact line. Such a model can be highly beneficial in interpreting experimental

data and planning new experiments. The numerical simulations of our model, complemented with analytic estimations, reveal the details of the rupture process. We show, e.g., that under some conditions several transient pores can open before the vesicle reaches its final state (either an SLB patch or a partially flattened vesicle). Our results are in good qualitative agreement with most of the available experimental data (of Andrecka et al. [8], in particular), justifying the legitimacy of the model. We demonstrate, e.g., that the larger the vesicle the more easily it ruptures and forms a bilayer. We also show that the rupture of vesicles can be very sensitive to their initial geometry (i.e., relative volume), which might explain why only a fraction of vesicles rupture immediately upon adsorption [3].

When a vesicle gets in contact with a flat hydrophilic surface it takes a cap-like shape [Fig. 1] to maximize its contact area with the surface [10, 11]. For strong adhesion (which is a prerequisite of rupture, as will be described later) the radius of curvature of the membrane at the contact line is very small (a few tens of nm). From now on we will consider vesicles that are significantly larger than this radius of curvature, thus, their shape can be well approximated by a perfect spherical cap. The surface tension of the membrane (σ) in thermal equilibrium is given by the Young-Dupre equation [12], which is the condition of force balance:

$$\sigma = \frac{W}{1+\cos\varphi} = W\frac{A_\parallel - \pi R^2}{2\pi R^2} \approx W\frac{A_0 - \pi R^2}{2\pi R^2}\,, \qquad (1)$$

where W is the adhesion energy between the membrane and the surface per unit area ($W > 0$ for attractive interaction); φ is the contact angle; R is the radius of the contact area; and $A_\parallel$ is the projected area of the vesicle (i.e., the area of its shape after averaging out the thermally induced membrane undulations), which is smaller than the total area of the membrane (A_0), but usually by only less than a few percent [12].

When a membrane pore forms (as a result of large surface tension), the surface tension drops down, allowing the contact line to propagate and to open the pore even further. At the same time, the vesicle loses volume via leakage through the pore, facilitating the resealing of the pore. These two competing effects lead to a non-trivial dynamics of the vesicles. Pore opening and closing were studied both experimentally [13] and theoretically [14] for a fixed contact area. Pore opening has an energy cost, because a free bilayer edge appears at its circumference. The line tension (λ) of the edge was deduced for various types of lipids from the pore dynamics of surface bound [15] and micropipette-aspirated [16] vesicles. It is typically of the order of 10 pN.

The propagation of the contact line was also observed experimentally [2, 5, 17]. It was studied at different lipid compositions [18] and in the presence of inhomogeneous, rough, or chemically structured surfaces [19, 20]. Contact line propagation was also taken into account in the coarse-grained Monte Carlo simulations of the surface kinetics of vesicles [21, 22].

Pore opening is an activated process [23], and can occur anywhere along the membrane. It will, however, be neglected at the contact area, where it is accompanied by the loss of adhesion energy. The energy of a pore of radius r can be written as [23, 24] $E = 2\pi r\lambda - \pi r^2\sigma$, where the first term is the energy contribution of the free edge, and the second term accounts for the energy gain due to the shrinkage of the membrane under surface tension σ. This energy function provides a parabolic barrier at radius $r^* = \lambda/\sigma$ with an activation energy of $E^* = \pi\lambda^2/\sigma$. Pore opening can thus be considered to occur at a rate of

$$k = k_0\frac{A_\mathrm{c}}{a^2}\exp\left(-\frac{\pi\lambda^2/\sigma}{k_\mathrm{B}T}\right)\,, \qquad (2)$$

where k_B is the Boltzmann constant, $T \approx 300$ K is the absolute temperature, $A_\mathrm{c} = A_0 - \pi R^2$ is the non-adhering surface area of the cap-shaped vesicle, a^2 is the surface area of a lipid molecule with linear size $a \approx 0.8$ nm [11], and k_0 is the local attempt rate of pore nucleation. We estimate it to be of the order of $k_0 \approx 10^8$ 1/s, which is consistent with the ns time scale of molecular diffusion at nm distances, and also with the molecular dynamics simulations of the formation and disappearance of a single file of water across a lipid bilayer [25]. Its exact value and even its exact order of magnitude are largely irrelevant, because pore opening becomes experimentally observable when the surface tension σ reaches the 10^{-3} N/m range, where the activation energy drops below $40\ k_\mathrm{B}T$ (about 100 kJ/mol), and thus an order of magnitude offset in k_0 can be compensated by only a 6% change in σ (about $2.3\ k_\mathrm{B}T$ change in the activation energy). Our estimation that the activation energy of pore opening has to drop below 100 kJ/mol for vesicle rupture to occur in the experimental time scale is in agreement with the reported 70 ± 8 kJ/mol [1] and 42 ± 4 kJ/mol [22] values for the activation energy of SLB formation. In our simulations whenever a pore opens (in a stochastic manner, at a rate of k) we set its radius a little larger than r^*. As pore formation is accompanied by the reduction of the surface tension, formation of a second pore is an unlikely event, therefore, we never allow more than one pore to be present at the same time.

We model the vesicle to always have a homogeneous surface tension σ along its entire surface (see the explanation later), and to always assume a cap shape (with cap radius R_c, cap height H_c, contact angle φ, and radius of contact area R), which together also ensure a homogeneous Laplace pressure of $2\sigma/R_\mathrm{c}$ inside the vesicle.

When a pore is present in the membrane (which can be anywhere along the non-adhering part of the cap, as long as it does not touch the contact line) the volume of the vesicle V changes as [13, 14, 26]

$$\dot{V} = -\frac{2}{3}\frac{r^3\sigma}{R_\mathrm{c}\eta_0} \qquad (3)$$

due to leakage driven by the internal Laplace pressure, where $\eta_0 \approx 10^{-3}$ Pa s denotes the viscosity of the aqueous medium.

The radius of the pore is governed by [13, 14]

$$\dot{r} = \frac{\sigma r - \lambda}{2\eta_\mathrm{m} d}\,, \qquad (4)$$

where $d \approx 5$ nm is the thickness of the bilayer [11], and $\eta_\mathrm{m} = 0.2$ Pa s is the viscosity of the membrane [24]. This equation

is valid as long as $r \ll R_{\rm c}$, which usually holds until the final stages of vesicle rupture. Pore closure occurs when the pore radius becomes zero.

The contact radius, irrespective of the presence of a membrane pore, propagates towards the Young-Dupre equilibrium at a rate

$$\dot{R} = \frac{W - (1+\cos\varphi)\sigma}{\eta_0 c_{\rm s}}\,, \tag{5}$$

where the surface drag coefficient $c_{\rm s}$ has several different components. Hydrodynamic friction of the aqueous medium has a contribution of the order of unity. Dimensional analysis suggests that the relative sliding between the two membrane layers (due to the smaller area of the inner layer) provides a more significant contribution of the order of $\eta_{\rm m}/\eta_0 \approx 200$, when the membrane is considered to be an isotropic viscous fluid, or $bd/\eta_0 \approx 100$, when the intermonolayer friction coefficient is taken as $b \approx 2\times10^7$ Pa s/m [27]. More detailed geometrical considerations provide an additional $(\pi-\varphi)$ cofactor at the contact line. Briefly, the reason for this cofactor is that each surface element at the highly curved cylindrical region of the contact line (characterized by a local radius of curvature $R_{\rm curv}$, and inclination angle φ^* with respect to the solid support) contributes to the drag force per unit length of the contact line by $\dot{R}\eta_{\rm m}\Delta\varphi^*$, obtained as the product of the velocity gradient across the membrane $\dot{R}/R_{\rm curv}$, the membrane viscosity $\eta_{\rm m}$, and the azimuthal arc length of the surface element $R_{\rm curv}\Delta\varphi^*$. The integral of φ^* from φ to π gives the cofactor $(\pi-\varphi)$. Similarly, an additional 2φ cofactor (for which the derivation is not detailed here) is provided by the non-adhering spherical cap region of the vesicle. These two cofactors together result in $c_{\rm s} \approx 1000$. Surface inhomogeneities and impurities can further increase the drag coefficient by many orders of magnitude. Therefore, in our simulations we explored a very broad range of $c_{\rm s}$ (see below).

The variables V, r, and R completely determine the geometry of the cap-shaped vesicle. The height of the cap $H_{\rm c}$ can be calculated from $V = \pi(3R^2H_{\rm c} + H_{\rm c}^3)/6$; the contact angle φ from $\cos\varphi = (R_{\rm c}-H_{\rm c})/R_{\rm c}$; the cap radius is $R_{\rm c} = (R^2+H_{\rm c}^2)/(2H_{\rm c})$; the projected area of the non-adhering part of the vesicle is $A_{\rm c\|} = 2\pi R_{\rm c}H_{\rm c} - \pi r^2$; whereas the total area of the non-adhering part (if the undulations along the strongly adhering contact area are neglected) is $A_{\rm c} = A_0 - \pi R^2$.

The three dynamical equations and the activated stochastic process of pore opening are coupled to each other by the surface tension of the membrane [28]:

$$\sigma = \frac{\pi^2\kappa}{a^2}\exp\left(-\frac{8\pi\kappa}{k_{\rm B}T}\alpha\right)\,, \tag{6}$$

where $\kappa \approx 10^{-19}$ J is the bending rigidity of the bilayer [29], and $\alpha = (A_{\rm c}-A_{\rm c\|})/A_{\rm c\|}$ denotes the strain of the membrane (the proportion of the surface area stored in the undulations). The apparent area expansion modulus can be expressed as $K = |{\rm d}\sigma/{\rm d}\alpha| = \sigma 8\pi\kappa/(k_{\rm B}T)$. For simplicity the elastic (Hookean) expansion of the bilayer is omitted, because it is negligible for small surface tensions and becomes comparable to the undulation driven expansion only at tensions relevant for pore opening [29]. The equilibration time of the surface tension can be estimated by dimensional analysis as $\tau_\sigma = \eta_0 R_0/K = \eta_0 R_0 k_{\rm B}T/(\sigma 8\pi\kappa)$, where the equivalent sphere radius R_0 is defined by $A_0 = 4\pi R_0^2$. τ_σ is smaller than any other relevant time scale of the dynamics, including the fastest time scale of pore closing: $\tau_r = 2\eta_{\rm m}dr^*/\lambda = 2\eta_{\rm m}d/\sigma$. The ratio $\tau_\sigma/\tau_r = (\eta_0/\eta_{\rm m})(R_0/d)k_{\rm B}T/(16\pi\kappa)$ is smaller than unity as long as the size of the vesicle (R_0) is smaller than about 1 mm, which holds in most experimental situations. Thus, the surface tension can indeed be considered homogeneous along the membrane.

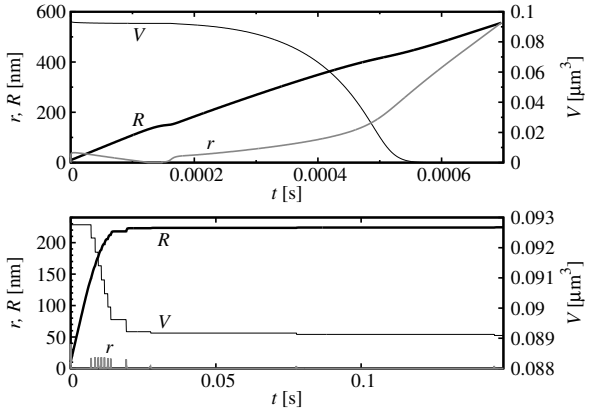

FIG. 2. Two examples of the time evolution of the three main geometrical variables (V, r, and R) for an initially spherical vesicle of size $R_0 = 280$ nm. System parameters are $\lambda = 10$ pN, $W = 10^{-3}$ N/m, $c_{\rm s} = 6\times10^3$ (top), $c_{\rm s} = 3\times10^5$ (bottom).

Using adaptive time steps we numerically simulated the model until either rupture (complete SLB formation) occurred or the time reached the observation time $\tau_{\rm obs} = 10^5$ s for two vesicle sizes (surface areas $A_0 = 100$ and 1 μm^2, or equivalent sphere radii $R_0 = 2.8$ μm and $R_0 = 280$ nm) and three line tensions ($\lambda = 20$, 10, and 5 pN). In each time step of the simulations the three main geometrical variables (V, r, and R) were updated according to the three dynamical equations, and if no pore was present in the membrane, pore opening was allowed to occur randomly at a rate k. The interaction potential was varied from weak ($W = 10^{-5}$ N/m) to strong ($W = 10^{-2}$ N/m) adhesion, and the surface drag coefficient from the (physically unattainable) hydrodynamic limit ($c_{\rm s} \approx 1$), through the membrane friction dominated range ($c_{\rm s} \approx 10^3$), up to very large, surface inhomogeneity governed values ($c_{\rm s} \approx 10^6$).

First, we investigated the dynamics of initially almost spherical vesicles (with a small contact radius of $R^{\rm init} = 10$ nm). Two qualitatively different examples of the time evolution of the three main geometrical variables (V, r, and R) can be seen in Fig. 2. The average rupture time $\langle\tau_{\rm rup}\rangle$ and the average number of pores opened $\langle N_{\rm pore}\rangle$ are shown in Figs. 3 and 4, respectively.

The most salient feature of the $\langle\tau_{\rm rup}\rangle$ data is that there is a sharp transition between fast rupture ($\langle\tau_{\rm rup}\rangle < 1$ s) and no observable rupture at all. Larger values of λ, as expected from

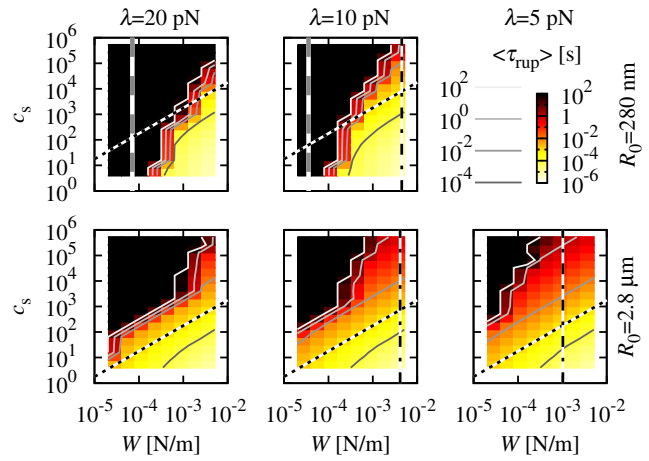

FIG. 3. The average time (based on 30 runs) needed for complete vesicle rupture (i.e., SLB formation) $\langle \tau_{\rm rup} \rangle$ as a function of W and $c_{\rm s}$, for two vesicle sizes: $R_0 = 280$ nm (top row), $R_0 = 2.8$ μm (bottom row); and three line tensions: $\lambda = 20$ pN (left column), $\lambda = 10$ pN (middle column), $\lambda = 5$ pN (right column). The data values are indicated by both color codes and contour lines (see the scales at the top right corner). The raggedness of the contour lines is an artifact of the discretization of the control parameters (W and $c_{\rm s}$). $W_{\rm crit}^{\rm therm}$, $W_{\rm crit}^{\rm pore}$, and $W_{\rm min}(1{\rm ms})$ are also plotted as gray dashed line, black dashed-dotted line, and black dotted line, respectively.

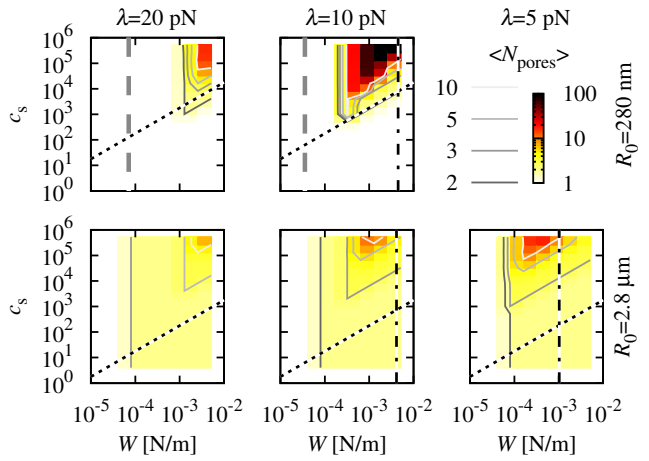

FIG. 4. The average number of pores opened $\langle N_{\rm pore} \rangle$ (until either rupture or time 10^5 s) for the same parameters as in Fig. 3.

its role in the activation energy of pore opening, make the rupture more difficult. The rupture process also has a noticeable size dependence. Thermodynamics dictates that rupture can occur only if the energy gain ($4\pi R_0^2 W$) due to adhesion is larger than the energy cost ($4\pi R_0 \lambda$) of the free edge of the final bilayer patch of radius $2R_0$ [11], i.e., if W is larger than the critical value

$$W_{\rm crit}^{\rm therm} = \lambda / R_0 \,, \tag{7}$$

which indeed depends reciprocally on the vesicle size (drawn as a gray dashed line, whenever it falls into the depicted parameter range).

Observable rupture, however, often occurs for significantly lager values of W than what the thermodynamic criterion suggests. This phenomenon can be understood from the pore opening kinetics. For a pore to open during the observation time $\tau_{\rm obs}$ the surface tension has to exceed the value (see Eq. (2))

$$\sigma_{\rm crit} = \frac{\pi \lambda^2}{k_{\rm B} T \ln(\tau_{\rm obs} k_0 A_0 / a^2)} \,. \tag{8}$$

For the small initial contact radius, the surface tension is much larger than this threshold value (see Eq. (1)), so the first pore opens rapidly. But if the pore reseals after the contact line has propagated, the surface tension can drop below the threshold. The worst case scenario is when the vesicle is almost flat ($\varphi \approx 0$) and $\sigma \approx W/2$. Pore opening for arbitrary geometry is, therefore, ensured only if W is larger than

$$W_{\rm crit}^{\rm pore} = 2\sigma_{\rm crit} \,, \tag{9}$$

illustrated as a black dashed-dotted line. Vesicle rupture for $W_{\rm crit}^{\rm therm} < W < W_{\rm crit}^{\rm pore}$ is, thus, not guaranteed, and depends on several factors, such as $c_{\rm s}$ or the initial geometry.

The initial geometry has indeed a dramatic effect on the vesicle's fate [Fig. 5]. Rupture cannot be observed if the initial surface tension, given by the Young-Dupre Eq. (1), is below $\sigma_{\rm crit}$, i.e., if W is smaller than

$$W_{\rm crit}^{\rm init} = \sigma_{\rm crit} \frac{2\pi {R^{\rm init}}^2}{A_0 - \pi {R^{\rm init}}^2} \,, \tag{10}$$

drawn as a gray dashed-dotted line.

Several contour lines in Figs. 3 and 4 run diagonally. The reason is that when a pore opens, the surface tension drops down, and the contact line propagates according to Eq. (5). Thus, a minimally necessary value of the adhesion energy to allow rupture within $\tau_{\rm rup}$ can be determined by replacing $\dot{R}$ with $2R_0/\tau_{\rm rup}$ and setting $\sigma = 0$ in Eq. (5):

$$W_{\rm min}(\tau_{\rm rup}) = 2R_0 \eta_0 c_{\rm s} / \tau_{\rm rup} \,, \tag{11}$$

which runs diagonally in the $W - c_{\rm s}$ parameter space. To guide the eye $W_{\rm min}(1{\rm ms})$ is plotted as a black dotted line.

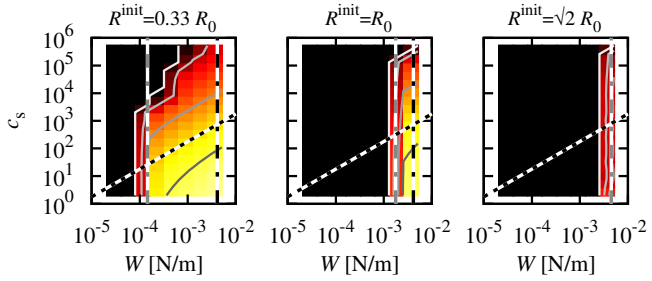

FIG. 5. The average rupture time for three initial geometries: $R^{\rm init} = 0.33 R_0$ (left), $R^{\rm init} = R_0$ (middle), $R^{\rm init} = \sqrt{2} R_0$ (corresponding to zero initial volume, right), for $R_0 = 2.8$ μm and $\lambda = 10$ pN. Colors and lines are as in Fig. 3. $W_{\rm crit}^{\rm init}$ is also drawn as a gray dashed-dotted line.

To sum up, vesicle rupture is guaranteed if $W > W_{\rm crit}^{\rm pore}$. It occurs rapidly for $W \gtrsim W_{\rm min}(1{\rm ms})$, and slowly, often accompanied by the appearance of several transient pores, otherwise. In the range $W_{\rm crit}^{\rm therm} < W < W_{\rm crit}^{\rm pore}$ the rupture process is highly sensitive to the initial geometry. Since the spherical shape is the most advantageous, we predict that vesicle fusion (leading to less spherical vesicles, e.g., $R^{\rm init} \approx 1.2R_0$ after the fusion of two identical spheres) cannot help SLB formation. This is consistent with the experiments by Andrecka et al. [8], who never observed any fusion events. Also, an osmotic shock that makes the surface bound vesicles more spherical is expected to facilitate SLB formation, as observed experimentally [3, 30]. The strong dependence of the vesicles' fate on their initial geometry also explains why some vesicles rupture immediately upon absorption, while others do not [3].

Note that we have not taken into account the fact that pore formation is more favorable near the contact line. Here the energy gain per unit area of the pore is larger than σ by W due to the high curvature of the membrane [12], which lowers the activation energy by a factor of $\sigma/(\sigma + W)$. This correction, however, is significant only when W is comparable to $\sigma_{\rm crit}$, so it facilitates vesicle rupture only when rupture is already guaranteed and, therefore, it has little effect on the results.

In conclusion, by combining the elastic theories of membranes, hydrodynamics, and the activated process of pore opening, we have developed a simple model of the dynamics (including the complete rupture) of lipid vesicles near solid surfaces. The model involves three ordinary differential equations (3-5) and a stochastic rate process [with a rate given by Eq. (2)], which are coupled to each other through the dependence of the surface tension on the geometry of the vesicle [as described by Eq. (6)]. The model relies on two basic but plausible assumptions (homogeneous surface tension, spherical cap shape), and a few simplifications (geometry independent drag coefficient, pore formation only at the non-adhering part of the membrane, undulations neglected at the contact area, omission of the elastic expansion of the membrane). Although the simplifications are expected to have little effect on the results, they are not inherent part of the model, and can be relaxed at will. The model provides the first detailed description of the dynamics of surface adhered lipid vesicles. Its predictions are consistent with most of the experimental observations (including the dependence of the rupture time on the size and initial geometry of the vesicle and also on the material properties of the solid support). The model also predicts some experimentally inaccessible behavior (such as the opening of transient pores), but most importantly, it provides a tool for determining under what conditions vesicle rupture and SLB formation is expected to occur. While the analytically determined criteria [from Eq. (7) to (11)] can serve as guidelines, in the experimentally relevant parameter range, where the cross-over between slow and rapid rupture takes place, the simulations of the model are indispensable.

ACKNOWLEDGMENTS

This work was supported by the Hungarian Science Foundation (grant K101436) and the European Union (grants EU-FP7-NMP-ASMENA and TAMOP 4.2.1/B-09/1/KMR-2010-0003).

[1] E. Reimhult, F. Höök, and B. Kasemo, Langmuir **19**, 1681 (2003).
[2] C. A. Keller, K. Glasmästar, V. P. Zhdanov, and B. Kasemo, Phys. Rev. Lett. **84**, 5443 (2000).
[3] J. M. Johnson, T. Ha, S. Chu, and S. G. Boxer, Biophys. J. **83**, 3371 (2002).
[4] I. Reviakine and A. Brisson, Langmuir **16**, 1806 (2000).
[5] S. Mornet, O. Lambert, E. Duguet, and A. Brisson, Nano Letters **5**, 281 (2005).
[6] I. Reviakine, F. F. Rossetti, A. N. Morozov, and M. Textor, J. Chem. Phys. **122**, 204711 (2005).
[7] K. L. Weirich, J. N. Israelachvili, and D. K. Fygenson, Biophys. J. **98**, 85 (2010).
[8] J. Andrecka, K. M. Spillane, J. Ortega-Arroyo, and P. Kukura, ACS Nano **7**, 10662 (2013).
[9] R. Richter, A. Mukhopadhyay, and A. Brisson, Biophys. J. **85**, 3035 (2003).
[10] R. Lipowsky and U. Seifert, Mol. Cryst. Liq. Cryst. **202**, 17 (1991).
[11] U. Seifert, Adv. Phys. **46**, 13 (1997).
[12] U. Seifert and R. Lipowsky, Phys. Rev. A **42**, 4768 (1990).
[13] O. Sandre, L. Moreaux, and F. Brochard-Wyart, P. Natl. Acad. Sci. USA **96**, 10591 (1999).
[14] F. Brochard-Wyart, P. G. De Gennes, and O. Sandre, Physica A **278**, 32 (2000).
[15] P.-H. Puech, N. Borghi, E. Karatekin, and F. Brochard-Wyart, Phys. Rev. Lett. **90**, 128304 (2003).
[16] D. V. Zhelev and D. Needham, BBA-Biomembranes **1147**, 89 (1993).
[17] R. P. Richter, R. Bérat, and A. R. Brisson, Langmuir **22**, 3497 (2006).
[18] C. Hamai, T. Yang, S. Kataoka, P. S. Cremer, and S. M. Musser, Biophys. J. **90**, 1241 (2006).
[19] P. S. Swain and D. Andelman, Phys. Rev. E **63**, 051911 (2001).
[20] Y. Roiter, M. Ornatska, A. R. Rammohan, J. Balakrishnan, D. R. Heine, and S. Minko, Nano Letters **8**, 941 (2008).
[21] V. P. Zhdanov, C. A. Keller, K. Glasmästar, and B. Kasemo, J. Chem. Phys. **112**, 900 (2000).
[22] K. Dimitrievski, E. Reimhult, B. Kasemo, and V. P. Zhdanov, Colloid. Surface. B **39**, 77 (2004).
[23] V. P. Zhdanov and B. Kasemo, Langmuir **17**, 3518 (2001).
[24] A. Diederich, G. Bähr, and M. Winterhalter, Langmuir **14**, 4597 (1998).
[25] S. J. Marrink, F. Jähnig, and H. J. C. Berendsen, Biophys. J. **71**, 632 (1996).
[26] J. Happel and H. Brenner, *Low Reynolds number hydrodynamics* (Martinus Nijhoff Publishers, 1983).
[27] P. Jonsson, J. P. Beech, J. O. Tegenfeldt, and F. Höök, Langmuir **25**, 6279 (2009).
[28] W. Helfrich and R.-M. Servuss, Il Nuovo Cimento D **3**, 137 (1984).
[29] E. Evans and W. Rawicz, Phys. Rev. Lett. **64**, 2094 (1990).
[30] H. Schönherr, J. M. Johnson, P. Lenz, C. W. Frank, and S. G. Boxer, Langmuir **20**, 11600 (2004).